

(B)

Primer name	Sequence (5' - 3')
RgB	CCATCGACGAGGACCAGTGGCAGAG
LB	GTTATCCGCCTGCTCGATCTTC
Rub-R	AGGCTATGCGATCAAGCTCAGGC

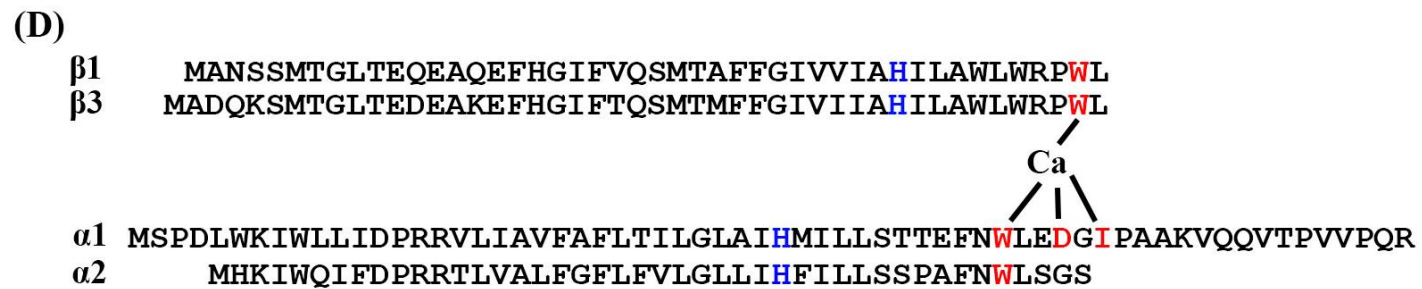
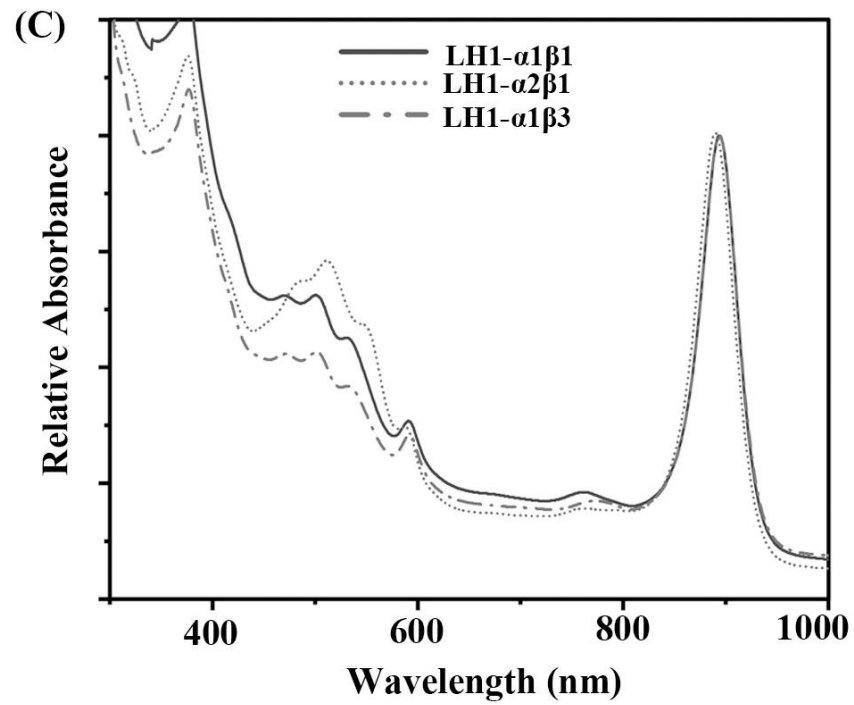


Fig. S1. Heterologous expression of the *Alc. tepidum* LH1-only complex. Schematic presentations of the arrangement of LH1–RC-encoding genes (*pufBALM*, *pufA*) from *Rsp. rubrum* and the *pufBA* from *Alc. tepidum* subsequent replacement in certain region of *puf* operon. Small arrows represent oligonucleotide primers used for PCR. **(B)** PCR primers used in this study. **(C)** Absorption spectrum of crude ICMs from the constructed strains. **(D)** Sequences of the LH1 polypeptides.

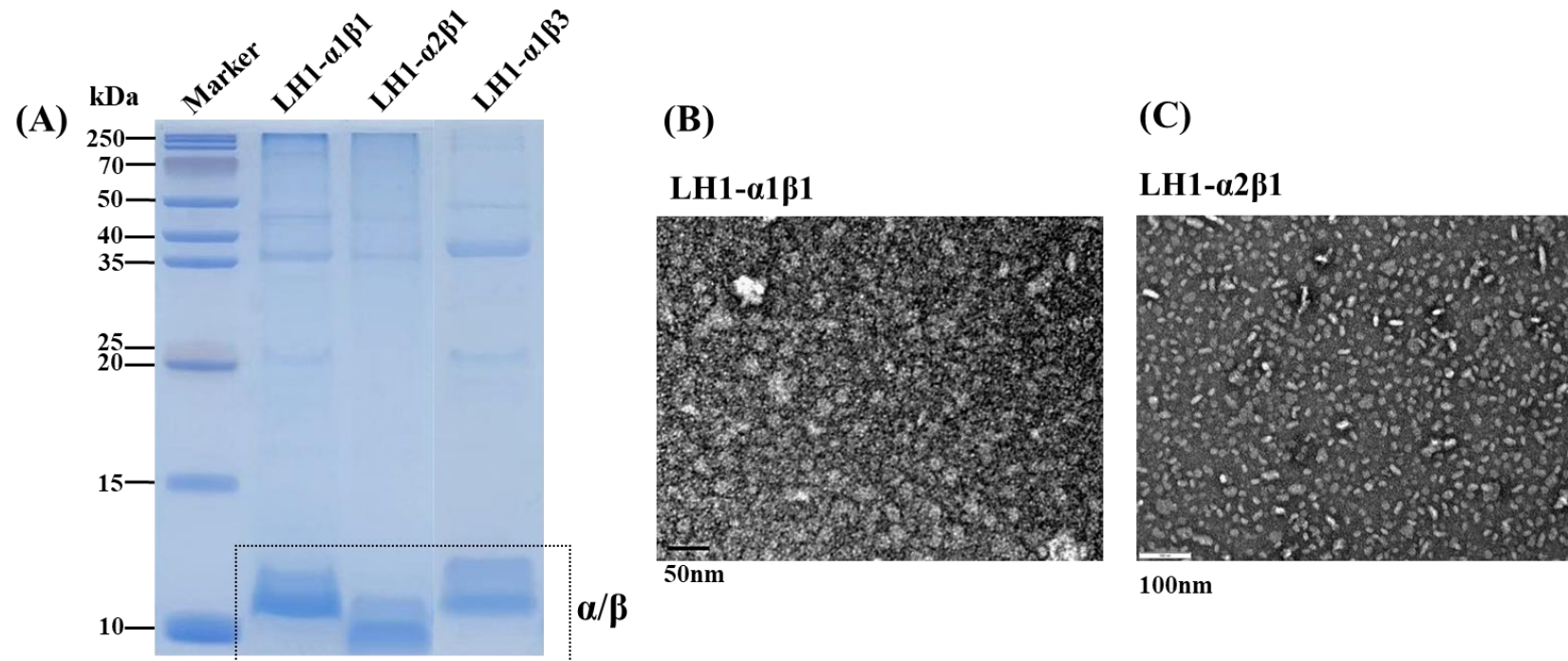


Fig. S2. Characterization of the *Alc. tepidum* LH1-only complexes obtained in this study. (A) SDS-PAGE of the purified LH1-only complexes, stained by Coomassie Brilliant Blue. (B)(C) A representative negatively stained electron micrograph of LH1- α 1 β 1 and LH1- α 2 β 1 with a concentration about \sim 0.04 mg/mL in 20 mM Tris-HCl (pH 7.5), 0.05% β -DDM.

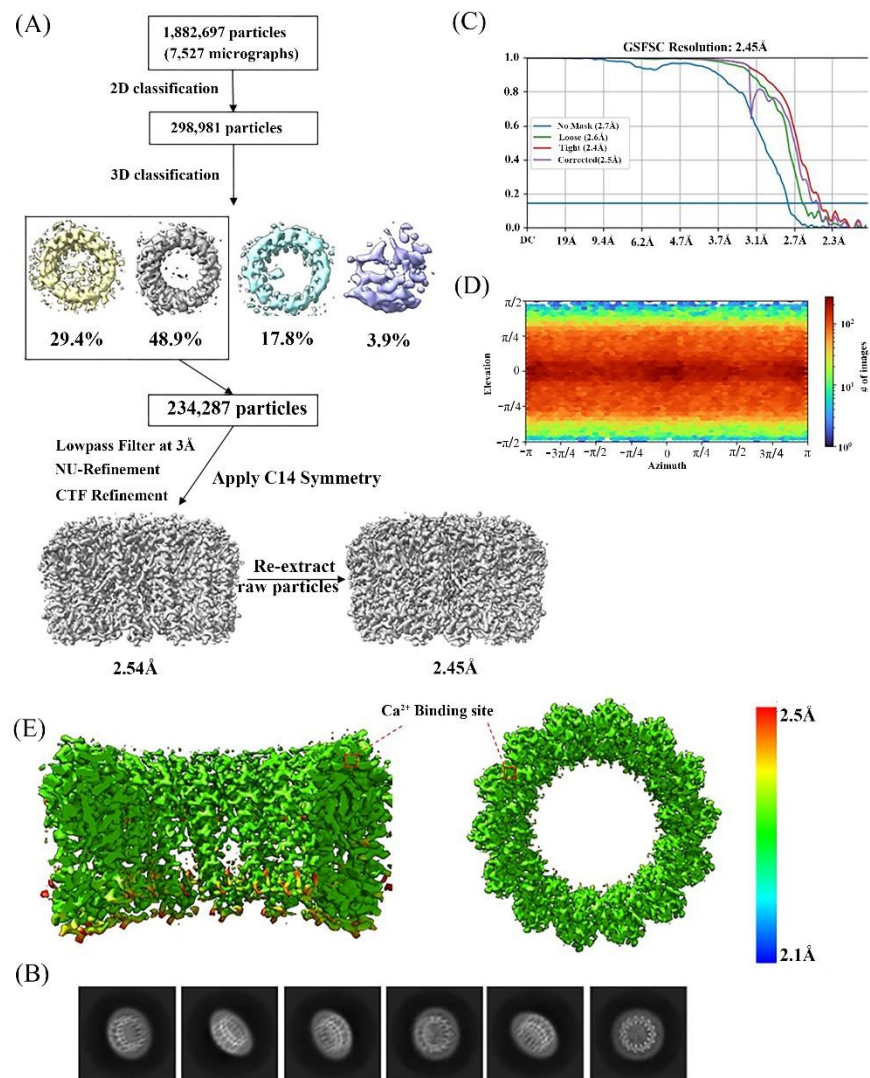


Fig. S3. Cryo-EM data process of the *Alc. tepidum* LH1- α 1 β 1 complex. (A) Image processing flow of 3D classification and reconstruction. Overview of cryo-EM data processing workflow for the *Alc. tepidum* LH1- α 1 β 1 complex dataset. Every major step is shown with the associated number of particles, percentage of particles per class, or estimated resolution. Selected 3D class that went into further processing is marked with rectangle. (B) Representative 2D class averages processed from micrograph of LH1- α 1 β 1 complex. (C) Gold standard Fourier shell correlation (FSC) plots of the cryo-EM map (unmasked: blue; loose masked: green; tight masked: red; corrected masked: purple) The Fourier shell correlation (FSC) plots of the cryo-EM map (unmasked: blue, loose masked: green, tight masked: red, corrected masked: purple) are superimposed. Global resolution values were calculated according to the gold-standard FSC=0.143. (D) Angular distribution of reconstructed particles. (E) Local resolution representation of the cryo-EM map of the LH1- α 1 β 1 complex from the side view and top view, respectively.

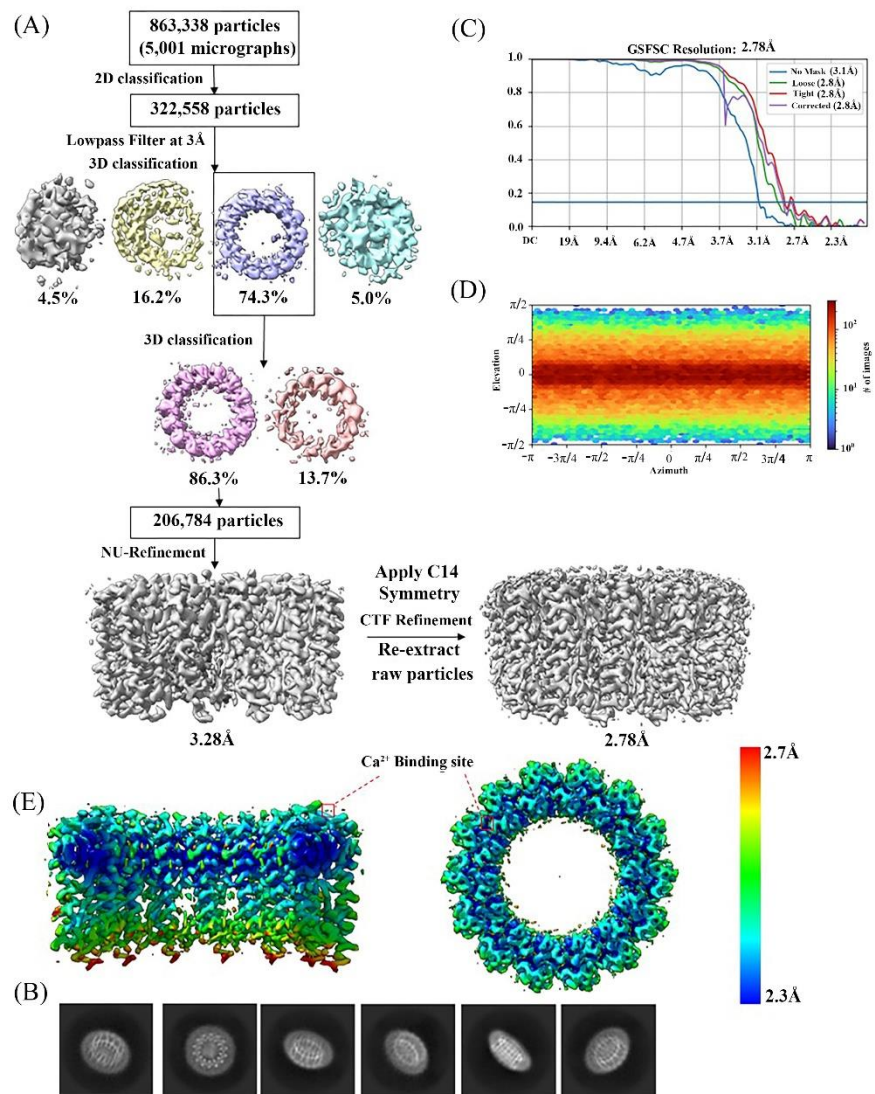


Fig. S4. Cryo-EM data process of the *Alc. tepidum* LH1- α 2 β 1 complex. (A) Image processing flow of 3D classification and reconstruction. Overview of cryo-EM data processing workflow for the *Alc. tepidum* LH1- α 2 β 1 complex dataset. Every major step is shown with the associated number of particles, percentage of particles per class, or estimated resolution. Selected 3D class that went into further processing is marked with rectangle. (B) Representative 2D class averages processed from micrograph of LH1- α 2 β 1 complex. (C) Gold –standard Fourier shell correlation (FSC) plots of the cryo-EM map (unmasked: blue; loose masked: green; tight masked: red; corrected masked: purple) are superimposed. Global resolution values were calculated according to the gold-standard FSC=0.143. (D) Angular distribution of reconstructed particles. (E) Local resolution representation of the cryo-EM map of the LH1- α 2 β 1 complex from the side view and top view, respectively.

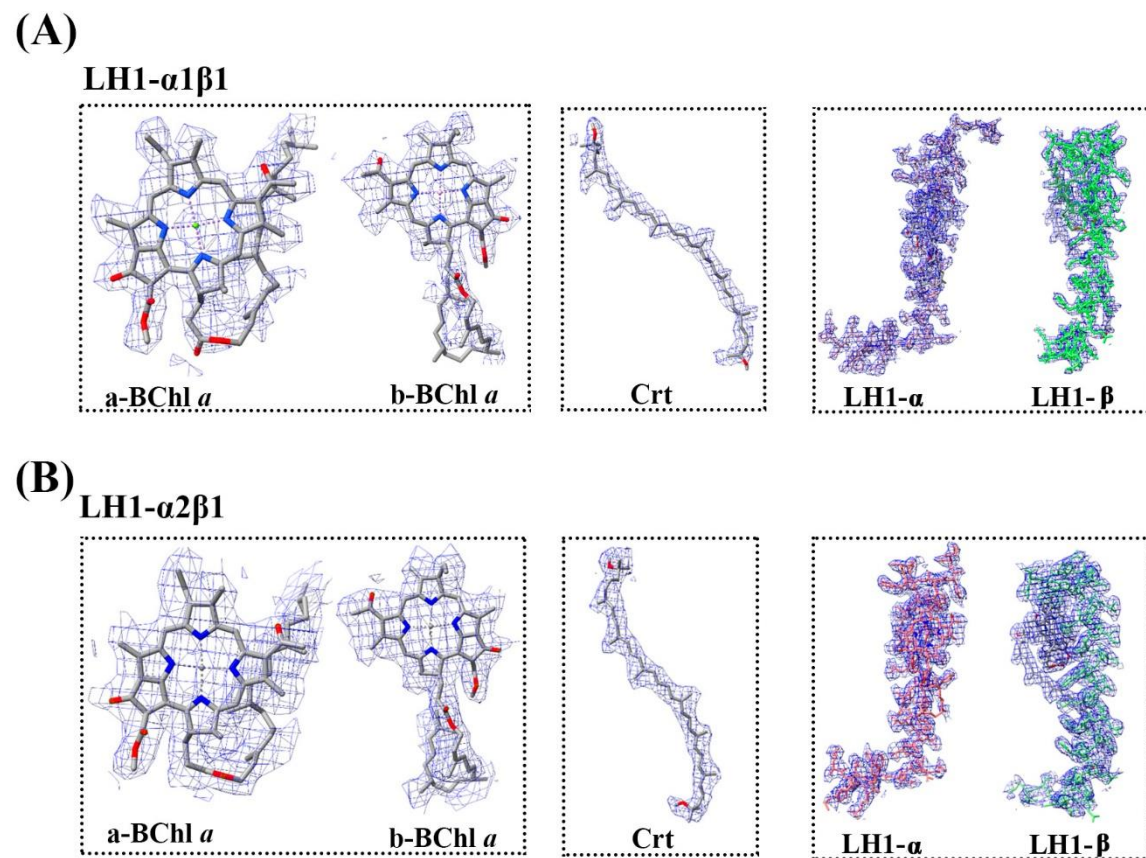


Fig. S5. Cryo-EM densities and structural models of the polypeptides in the *Alc. tepidum* LH1-only complexes. The density maps of LH1- α 1 β 1 (A) and LH1- α 2 β 1 (B) are shown at a contour level of 4.0 σ .

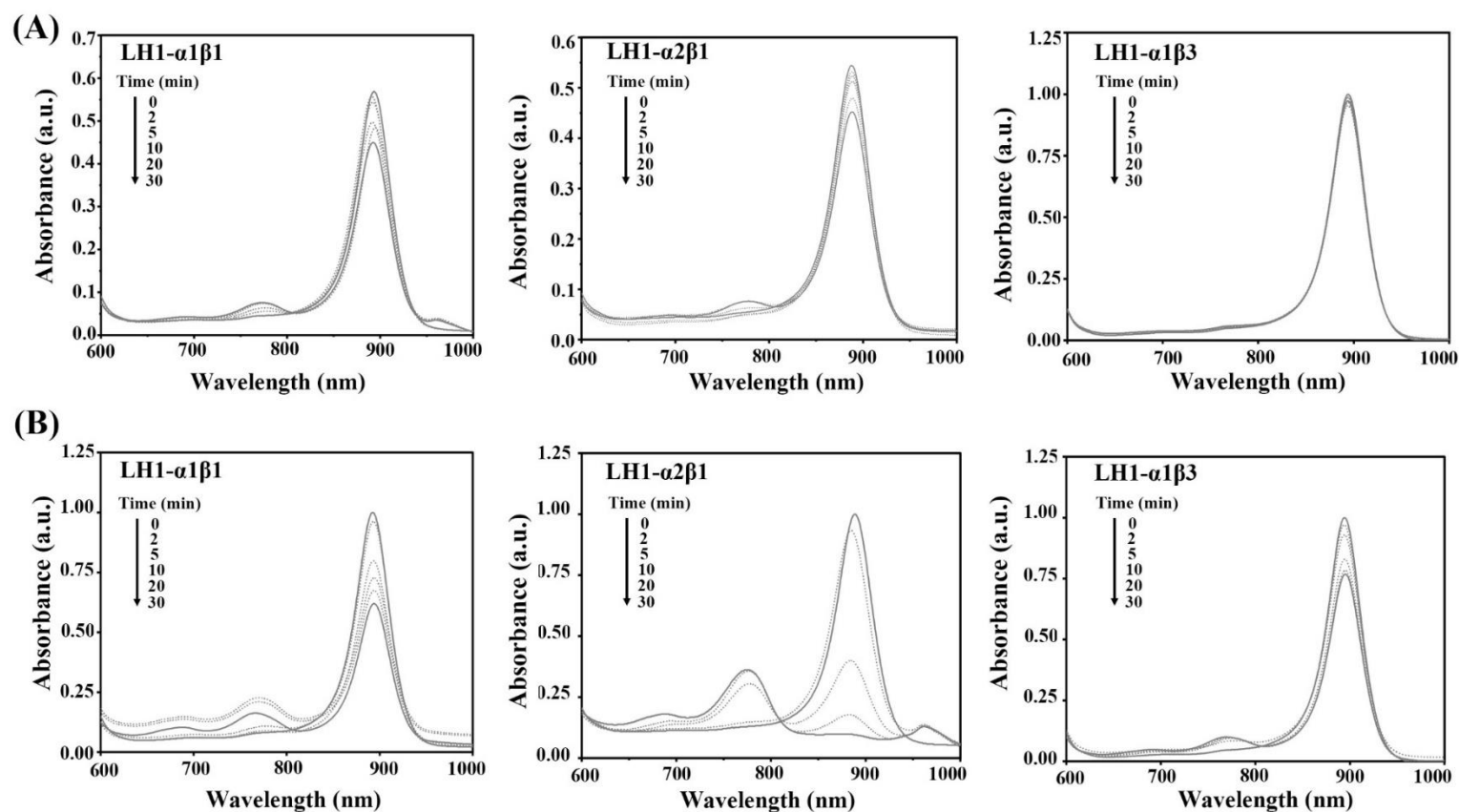


Fig. S6. Changes in the absorption spectra on thermal degradation at 65 °C (A) and 75 °C (B) for the *Alc. tepidum* LH1-only complexes. From left to right: LH1- $\alpha 1\beta 1$, LH1- $\alpha 2\beta 1$ and LH1- $\alpha 1\beta 3$, respectively. The samples were dissolved in 20 mM Tris-HCl (pH 7.5) and 0.03 % (w/v) β -DDM.